ACS Catalysis

Open Access

pubs.acs.org/acscatalysis

Research Article

Photoelectrochemical Synthesis of Benzo[*b*]phosphole Oxides via Sequential P−H/C−H Bond Functionalizations

Nayan Saha and Burkhard König*

Cite This: *ACS Catal.* 2024, 14, 17958−17971

Read Online

ACCESS | Metrics & More | Article Recommendations | Supporting Information

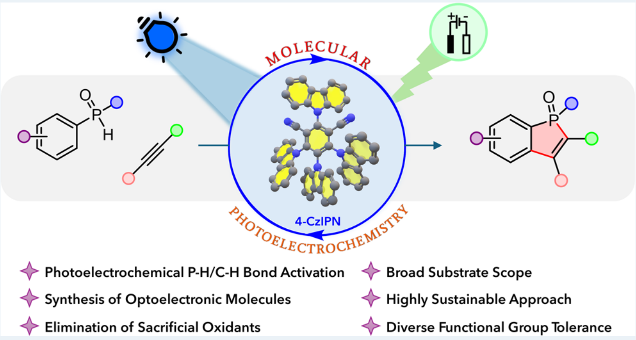

ABSTRACT: Benzo[*b*]phosphole oxides are important *P*-heterocycles that find applications in optoelectronics due to their inherent photophysical properties. Traditional routes for the synthesis of such molecules from readily available precursors require stoichiometric amounts of transition metal salts, bases, oxidants, and additives, thereby lacking efficiency. Photochemical pathways still need a terminal oxidant to complement the photocatalytic cycle, whereas electricity may be a viable oxidant. Hence, photoelectrochemistry (PEC), combining photocatalysis and synthetic organic electrochemistry, was used to simplify the synthetic protocols. We use the potency of 4CzIPN for the consecutive P−H/C−H bond functionalizations for preparing benzo[*b*]phosphole oxides from secondary phosphine oxides and nonactivated internal alkynes with up to 93% yields and with good functional group tolerance. Detailed mechanistic investigations confirm an intermolecular electron transfer between 4CzIPN and aryl secondary phosphine oxides upon photoexcitation. The photocatalyst is regenerated by anodic oxidation.

KEYWORDS: *photoelectrochemistry, organocatalysis, annulation, photoredox, C−P bond formation*

■ INTRODUCTION

Organophosphorus compounds are important organic compounds found in the skeletal framework of DNA with phosphodiester bonds and phospholipids, various insecticides, and warfare agents.[1] Among them, phosphorus heterocycles find application in synthesis, pharmaceuticals, and material science.[2] Benzo[*b*]phosphole, the P-analogue of indole, and its derivatives are widely applied in photovoltaics, organic optoelectronic materials, and bioimaging probes. The tetrahedral geometry of the phosphorus atom in π-conjugated ring systems results in $\sigma^*-\pi^*$ interactions which lowers the energy of the lowest unoccupied molecular orbital (LUMO) giving rise to unique electronic and photophysical properties.[3] Typical approaches for the synthesis of benzo[*b*]phosphole oxides start with prefunctionalized substrates such as alkynylphosphine oxides which are treated with stoichiometric quantities of a strong base and transition metal catalysts.[4] Recent reports show that this transformation can be achieved by intermolecular oxidative annulation protocols, employing secondary phosphine oxides and internal alkynes with considerably excess amounts of transition-metal-based oxidants, strong bases, and additives (Scheme 1).[5] Depicting a plausible mechanism reveals a radical pathway that initiates with the formation of phosphinoyl radicals upon oxidation of the secondary phosphine oxides by sacrificial Mn(III)-, Cu(II)-, Ag(I)-based or non-metal-based oxidants at typically high temperatures. Phosphinoyl radicals react with alkynes to produce alkenyl radicals, whose fate lies in the intramolecular addition step. Subsequent oxidation and deprotonation furnishes the benzo[*b*]phosphole oxide products. However, these protocols are limited in their functional group tolerance and the substrate scope.

Current reports have shown that the addition of phosphinoyl radicals to alkynes is feasible at room temperature and high temperature is only required for the generation of the former by different oxidants.[6] Lakhdar et al. used Eosin Y as a photocatalyst in an oxidative quenching cycle to reduce an organic oxidant, which in turn generates its active form to perform HAT with phosphine oxides producing the phosphinoyl radical.[7] This protocol avoids the use of metal oxidants but still requires stoichiometric amounts of an organic oxidant, base, and rather long reaction time.

Photoredox catalysis (PRC) has enabled researchers to explore otherwise challenging reactions in simpler ways by harnessing the power of the energy from photons, thereby transforming it into chemical potential.[8] The excited state of a

Received: October 13, 2024
Revised: November 13, 2024
Accepted: November 13, 2024
Published: November 20, 2024

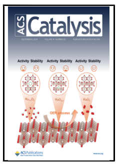

https://doi.org/10.1021/acscatal.4c06292
ACS Catal. 2024, 14, 17958−17971

Scheme 1. Importance of Organophosphorus Chemistry and Benzophospholes, Conventional Routes toward Benzophosphole Oxides, Organic Photoelectrochemistry (PEC), and Our Approach

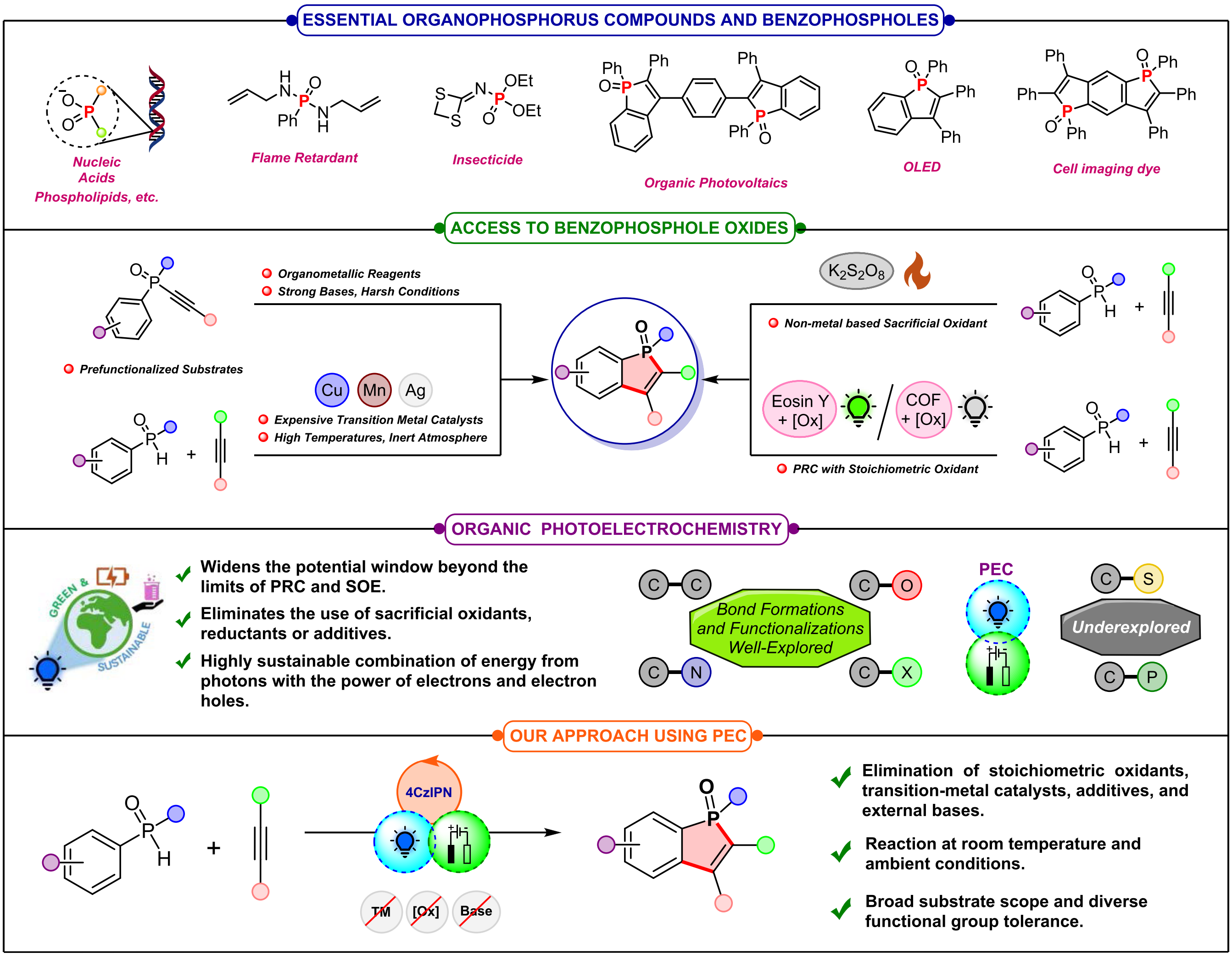

photocatalyst serves as the juncture of multiple kinetic processes occurring within a span of picoseconds to seconds by changing electronic configurations.[9] On the other hand, synthetic organic electrochemistry (SOE)[10] serves as an efficient tool in organic reactions, to avoid stoichiometric sacrificial oxidants or reductants utilizing electrical energy to create a pool of electrons and electron holes.[11] Independently PRC and SOE being extensively studied are also associated with some drawbacks. To utilize the advantage of PRC, and to expand the operational redox window of SOE, organic photoelectrochemistry (PEC) has been established (Scheme 1).[12]

We perceived that the route toward the synthesis of structurally diverse benzo[*b*]phosphole oxides might be made more economical and sustainable by PEC. Hence, we hypothesized the use of 4CzIPN as the molecular organophotocatalyst for the intermolecular single electron transfer to generate phosphinoyl radicals from secondary phosphine oxides under blue light irradiation. To eliminate the sacrificial terminal oxidants and stoichiometric amounts of additives as used in previous reports[13] for this synthetic transformation, we instead used electricity for the oxidation steps in the transformation making the methodology more efficient and simpler.

■ RESULTS AND DISCUSSION

Our investigations commenced by employing diphenylphosphine oxide **1a** and diphenylacetylene **2a** as the model substrates. We electrolyzed a solution of 0.2 mmol of **2a** with 2 equiv of **1a**, 5 mol % of 4CzIPN (**PC$_1$**), and 1 equiv of tetrabutylammonium hexafluorophosphate (TBAPF$_6$) as the conducting electrolyte in 4 mL of MeCN using an undivided cell at a constant voltage (CV) of +1.8 V under the irradiation of blue light (456 nm Kessil lamp).

Employing graphite electrodes as both cathode and anode, only 27% of the desired product **3a** was achieved after 3 h (Table 1, entry 1). On changing the solvent from MeCN to DMF, we observed an increase in the yield of **3a** to 42% (Table 1, entry 2). We found no significant improvement when we varied the solvent to MeOH, MeCN-H$_2$O, and MeCN-MeOH (see SI). We also planned to incorporate mild bases such as NaHCO$_3$, K$_3$PO$_4$, and Et$_3$N, but failed to observe any remarkable benefit for the reaction (see the SI). On employing graphite as the anode and Pt foil as the cathode, in MeCN, we obtained around 20% of **3a** (Table 1, entry 3). Nonetheless, we saw substantially lower yields using solvent mixtures like DMF-H$_2$O, DMF-MeOH, and MeCN-MeOH (Table 1, entries 4−6). Shifting the solvent to DMA enhanced the yield of **3a** to 68% (Table 1, entry

Table 1. Optimization of the Reaction Conditions for Photoelectrochemical P−H/C−H Functionalizations[a]

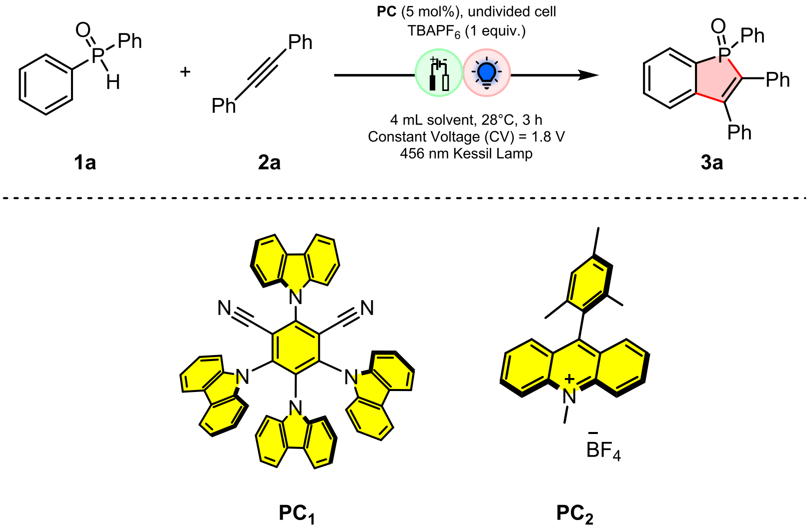

entry	electrodes (+|−)	solvent	yield (%)[b]
1	graphite|graphite	CH_3CN	27
2	graphite|graphite	DMF	42
3	graphite|Pt	CH_3CN	20
4	graphite|Pt	DMF:H_2O = 4:1 (v/v)	34
5	graphite|Pt	DMF:MeOH = 4:1 (v/v)	18
6	graphite|Pt	CH_3CN:H_2O = 4:1 (v/v)	19
7	graphite|Pt	DMA	68
8	**graphite|Pt**	**DMF**	**93**
9[c]	graphite|Pt	DMF	10
10[d]	graphite|Pt	DMF	14
11[e]	graphite|Pt	DMF	8
12[f]	graphite|Pt	DMF	5

[a] Standard reaction condition unless otherwise specified: **1a** (0.4 mmol), **2a** (0.2 mmol), **PC$_1$** (5 mol %), $TBAPF_6$ as electrolyte (1.0 equiv), solvent (4 mL), light irradiation from 456 nm Kessil lamp, electrolysis by using constant voltage (CV) of +1.8 V in an undivided cell equipped with anode (+) and cathode (−) for 3 h. [b] Yield determined by gas chromatography with reference to benzophenone as internal standard. [c] Using **PC$_2$** instead of **PC$_1$**. [d] No electricity. [e] In dark. [f] No **PC$_1$**.

7). Notably on using only DMF as the solvent, to our delight, we observed a significant increase in the yield of **3a** to 93% (Table 1, entry 8) at a constant voltage of +1.8 V for 3 h (2.4 F/mol). We also explored the well-known Mes-Acr$^+$ (**PC$_2$**) as the photocatalyst, but it furnished only 10% of **3a** (Table 1, entry 9) under our condition. The significant roles of electricity, light, and the presence of a photocatalyst were confirmed by control experiments in their absence under the standard PEC conditions, yielding only 14, 5, and 8% of **3a**, respectively (Table 1, entries 10−12).

With the optimized conditions of the photoelectrochemical protocol, we explored the substrate scope. We applied the PEC protocol to a series of substituted secondary diarylphosphine oxides, alkyl arylphosphine oxides, and alkyl arylphosphinates (Table 2) to test for the tolerance of the presence of various functional groups.

The unsubstituted product **3a** was isolated in 87% yield under the optimized reaction conditions. Secondary phosphine oxides with bisfunctionalized aryl rings gave rise to the formation of regioisomeric benzo[*b*]phosphole oxides in most cases. We tried the PEC protocol on compounds bearing the electron-donating Me groups in the C4- and C2-positions of the *P*-aryl rings, and the reaction proceeded smoothly delivering regioisomeric mixtures **3b**, **3b′** (2.5:1) and **3c**, **3c′** (1:2.5) in 92 and 78% yields, respectively (ratio of regioisomers calculated from ^{31}P NMR). The bis-3,5-diMe-substituted secondary phosphine oxide furnished 88% **3d** as an exclusive product. *tert*-Butyl substitution in the C4-position was well tolerated and gave **3e**, **3e′** (1:0.8) in 86% yield. Electron-withdrawing C4-halo (4-Cl and 4-F) substitution provided the respective regioisomeric products **3f**, **3f′** (1:0.6) and **3g**, **3g′** (1:0.54) in good yields of 82 and 74%, respectively. The products can be further functionalized in cross-coupling reactions. The presence of electron-rich bis-4-methoxy and bis-2-methoxy substitutions on the *P*-aryl rings gave products **3h**, **3h′** (1:0.6) and **3i**, **3i′** (1:6) in 89 and 73% yields, respectively. The electron-deficient bis-4-trifluoromethyl-substituted diphenylphosphine oxide was found to be amenable under our conditions and delivered 72% of **3j**, **3j′** (1:0.4). Di-α-naphthyl and di-β-naphthylphosphine oxides were converted in our protocol furnishing 68% of **3k** and 75% of **3l**, **3l′** (1:0.3), respectively.

Ethyl phenylphosphinate was employed in our protocol (Table 3) with various alkynes and found suitable for the PEC conditions furnishing moderate to excellent yields of the desired products (**3m**, 79%; **3n**, 81%; **3o**, 77%; **3p**, 74%). Furthermore, alkyl arylphosphine oxides were reacted. Methyl phenyl phosphine oxide and ethylphenyl phosphine oxides reacted with diphenylacetylene and di-*p*-tolylacetylenes affording the corresponding products in very good yields respectively (**3q**, 82%; **3r**, 85%; **3s**, 79%; **3t**, 80%). Diphenylphosphine sulfide

Table 2. Substrate Scope for the Photoelectrochemical Dehydrogenative Annulation with Various Substituted Diarylphosphine Oxides[a,b]

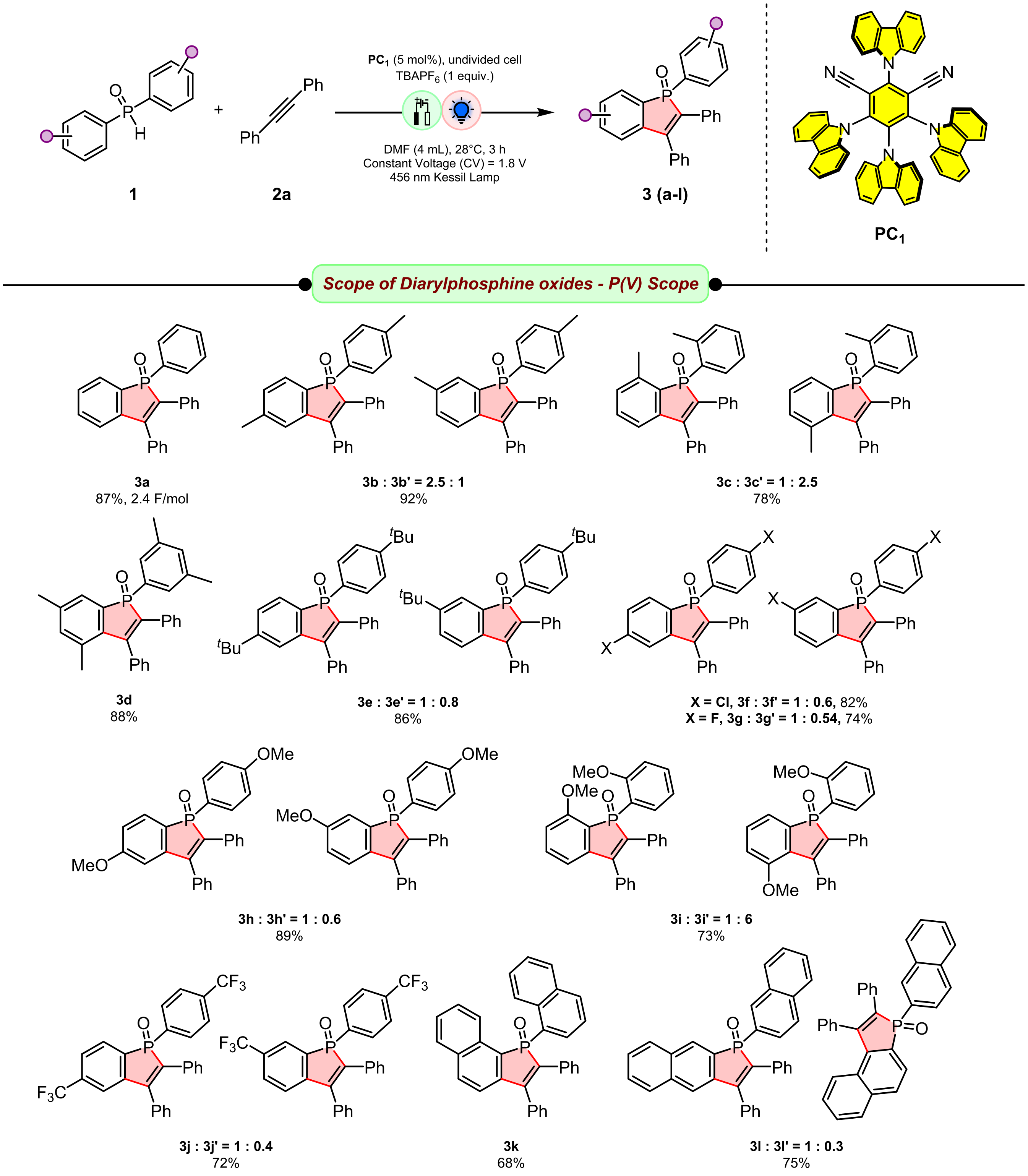

[a] Standard reaction condition unless otherwise specified: **1** (0.4 mmol), **2a** (0.2 mmol), **PC$_1$** (5 mol %), TBAPF$_6$ as electrolyte (1.0 equiv), DMF (4 mL), light irradiation from 456 nm Kessil lamp, electrolysis by using constant voltage (CV) of +1.8 V in an undivided cell equipped with a graphite anode (+) and a Pt foil cathode (−) for 3 h. [b] Isolated yield of two successive batches.

reacted in the PEC protocol, giving the products **3u** in 61% yield and **3v** in 67% yield.

Next, we explored the reactions of nonactivated internal alkynes in our scheme and started with symmetrical alkynes (Table 4). The reactions of 1,2-di-*p*-tolylethyne and 1,2-bis(4-ethylphenyl)ethyne yielded the products **4a** (93%) and **4b** (86%). Electron-rich 1,2-bis(4-methoxyphenyl)ethyne produced **4c** in 82% yield, while the electron-deficient halo

Table 3. Substrate Scope for the Photoelectrochemical Dehydrogenative Annulation with Ethyl Phenylphosphinate, Alkyl Arylphosphine Oxides, and Diphenylphosphine Sulfide[a,b]

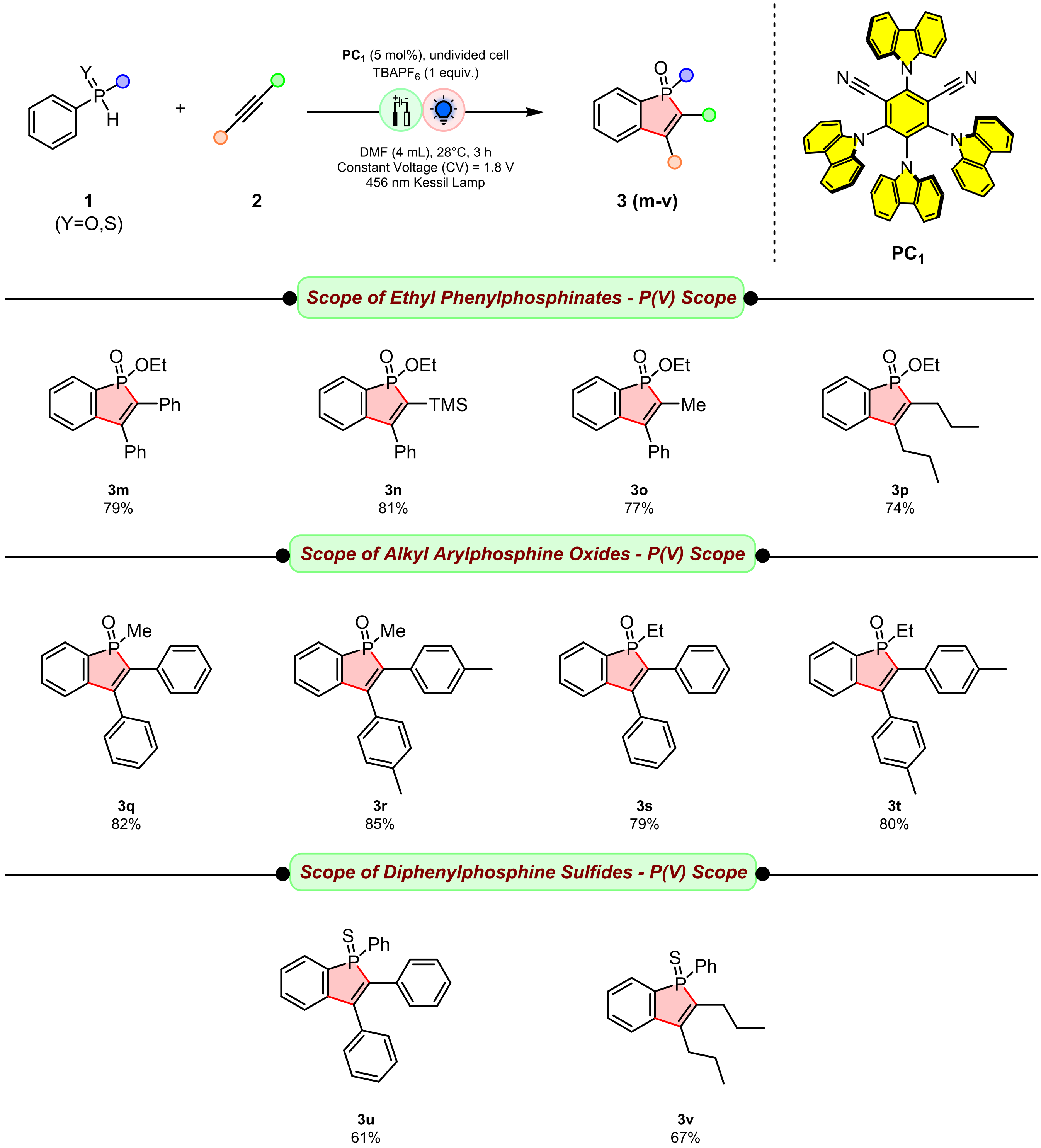

[a] Standard reaction condition unless otherwise specified: **1** (0.4 mmol), **2** (0.2 mmol), **PC$_1$** (5 mol %), TBAPF$_6$ as electrolyte (1.0 equiv), DMF (4 mL), light irradiation from 456 nm Kessil lamp, electrolysis by using constant voltage (CV) of +1.8 V in an undivided cell equipped with a graphite anode (+) and a Pt foil cathode (−) for 3 h. [b] Isolated yield of two successive batches.

derivatives 1,2-bis(4-fluorophenyl)ethyne, 1,2-bis(4-chlorophenyl)ethyne, and 1,2-bis(4-bromophenyl)ethyne gave the respective benzo[*b*]phosphole oxide products **4d** in 71%, **4e** in 83%, and **4f** in 78% yield, respectively. 1,2-Bis(4-(trifluoromethyl)phenyl)ethyne, bearing strongly electron-withdrawing trifluoromethyl substituents, furnished **4g** in an excellent yield of 89%. Employing 1,2-bis-(diphenylphosphaneyl)ethyne as the alkyne partner, we obtained 71% of oxidized product **4h**. 4-Octyne was well tolerated under our conditions and gave 75% of product **4i**. 1,2-

Table 4. Substrate Scope for the Photoelectrochemical Dehydrogenative Annulation with Various Symmetrical Internal Alkynes[a,b]

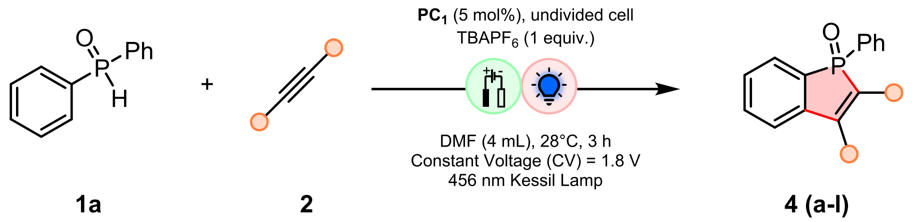

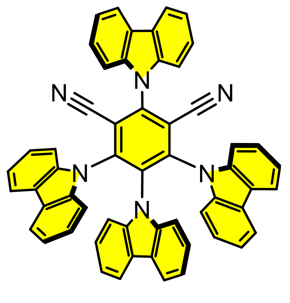

PC_1

Scope of Symmetrical Internal Alkynes

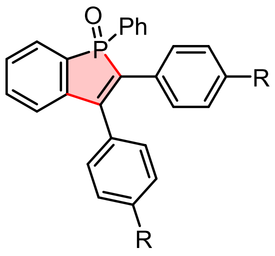

4a, R=Me, 93%
4b, R=Et, 86%

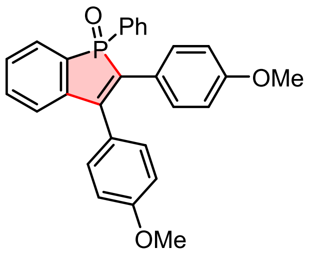

4c, 82%

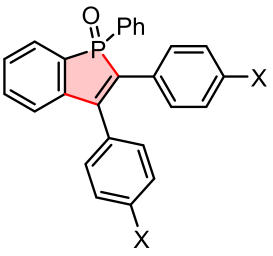

4d, X=F, 71%
4e, X=Cl, 83%
4f, X=Br, 78%

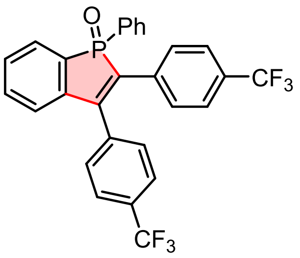

4g, 89%

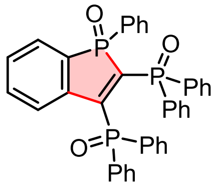

4h, 71%

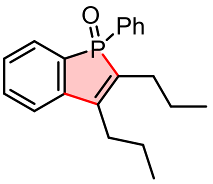

4i, 75%

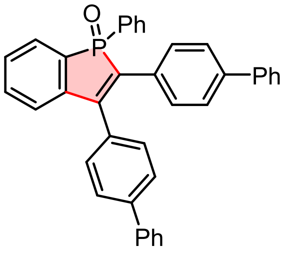

4j, 89%

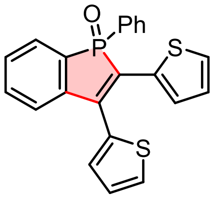

4k, 84%

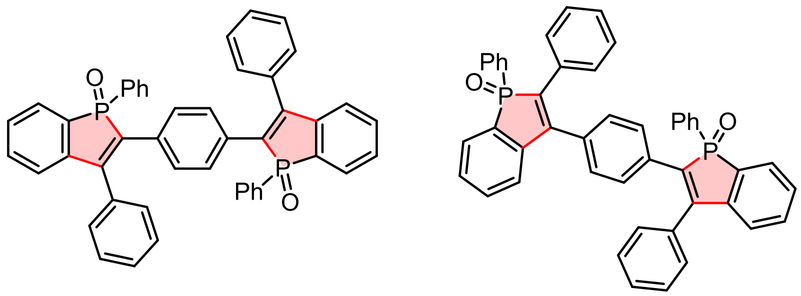

4l : 4l' = 1 : 0.54
78%

[a] Standard reaction condition unless otherwise specified: **1a** (0.4 mmol), **2** (0.2 mmol), $\mathbf{PC_1}$ (5 mol %), $TBAPF_6$ as electrolyte (1.0 equiv), DMF (4 mL), light irradiation from 456 nm Kessil lamp, electrolysis by using constant voltage (CV) of +1.8 V in an undivided cell equipped with a graphite anode (+) and a Pt foil cathode (−) for 3 h. [b] Isolated yield of two successive batches.

Di([1,1′-biphenyl]-4-yl)ethyne resulted in product **4j** in a very good yield of 89%. 1,2-Di(thiophen-2-yl)ethyne was amenable under the PEC conditions and delivered product **4k** in 84% yield. Surprisingly, using the diyne 1,4-bis(phenylethynyl)-benzene resulted in bisannulation using the double amount of diphenylphosphine oxide to furnish products **4l**, **4l'** (1:0.54) in 78% yield.

After exploring the tolerability of symmetrical alkynes, we moved on to study the substrate spectrum by employing a series of unsymmetrical alkynes (Table 5). We began with prop-1-yn-1-ylbenzene and but-1-yn-1-ylbenzene as the annulation

https://doi.org/10.1021/acscatal.4c06292
ACS Catal. 2024, 14, 17958−17971

Table 5. Substrate Scope for the Photoelectrochemical Dehydrogenative Annulation with Various Unsymmetrical Internal Alkynes[a,b]

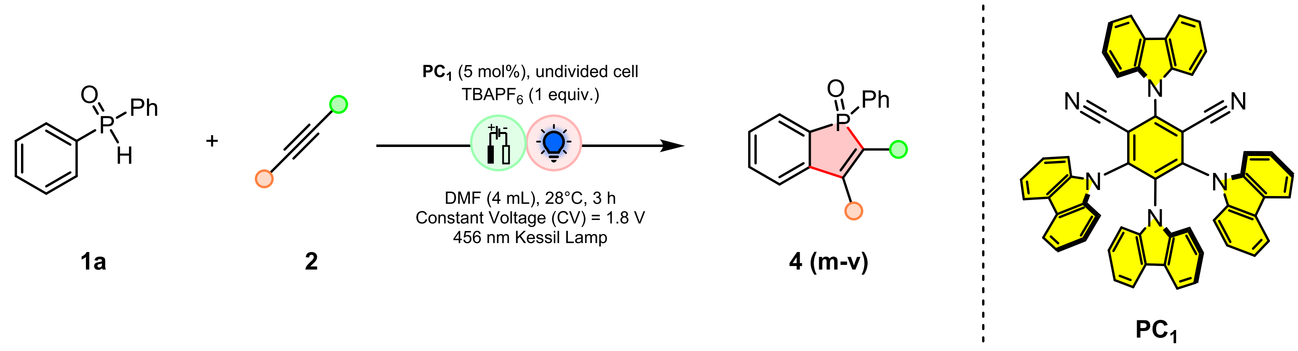

Scope of Unsymmetrical Internal Alkynes

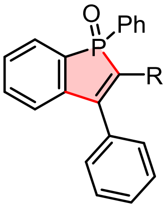

4m, R=Me, 86%
4n, R=Et, 82%

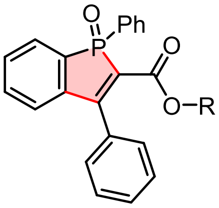

4o, R=Me, 61%
4p, R=Et, 67%

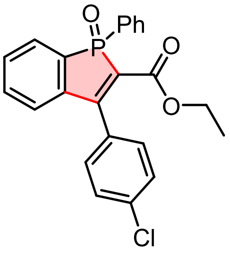

4q, 69%

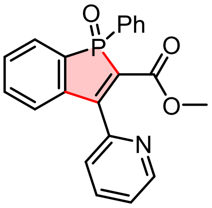

4r, 56%

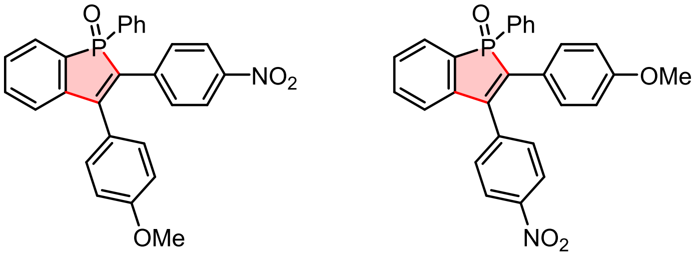

4s : 4s' = 1 : 0.84, 57%

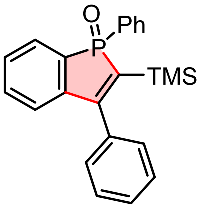

4t, 84%

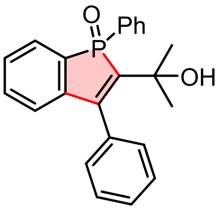

4u, 68%

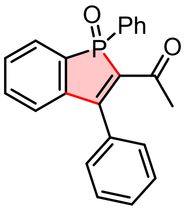

4v, 74%

[a] Standard reaction condition unless otherwise specified: **1a** (0.4 mmol), **2** (0.2 mmol), **PC_1** (5 mol %), $TBAPF_6$ as electrolyte (1.0 equiv), DMF (4 mL), light irradiation from 456 nm Kessil lamp, electrolysis by using constant voltage (CV) of +1.8 V in an undivided cell equipped with a graphite anode (+) and a Pt foil cathode (−) for 3 h. [b] Isolated yield of two successive batches. Reaction proceeds with good regioselectivity, only for compound **4s**, a mixture of regioisomers is obtained.

partners and obtained a very good yield of the products **4m** and **4n** in 86 and 82%, respectively. Employing the methyl and ethyl esters of 3-phenylpropiolic acid, we were able to isolate the respective products in moderate yields (**4o**, 61%; **4p**, 67%). Ethyl 3-(4-chlorophenyl)propiolate and methyl 3-(pyridin-2-yl)propiolate were also tolerated well and delivered the products (**4q**, 69%; **4r**, 56%). A combination of both electron-donating and -withdrawing substituents was present in the alkyne, 1-methoxy-4-((4-nitrophenyl)ethynyl)benzene which furnished the regioisomeric products **4s, 4s′** (1:0.84) in 57% yield. Trimethyl(phenylethynyl)silane gave an excellent yield of 84% of product **4t** in our PEC protocol. In addition, tertiary

Scheme 2. Scale-Up Reactions and Radical Inhibition Studies[a]

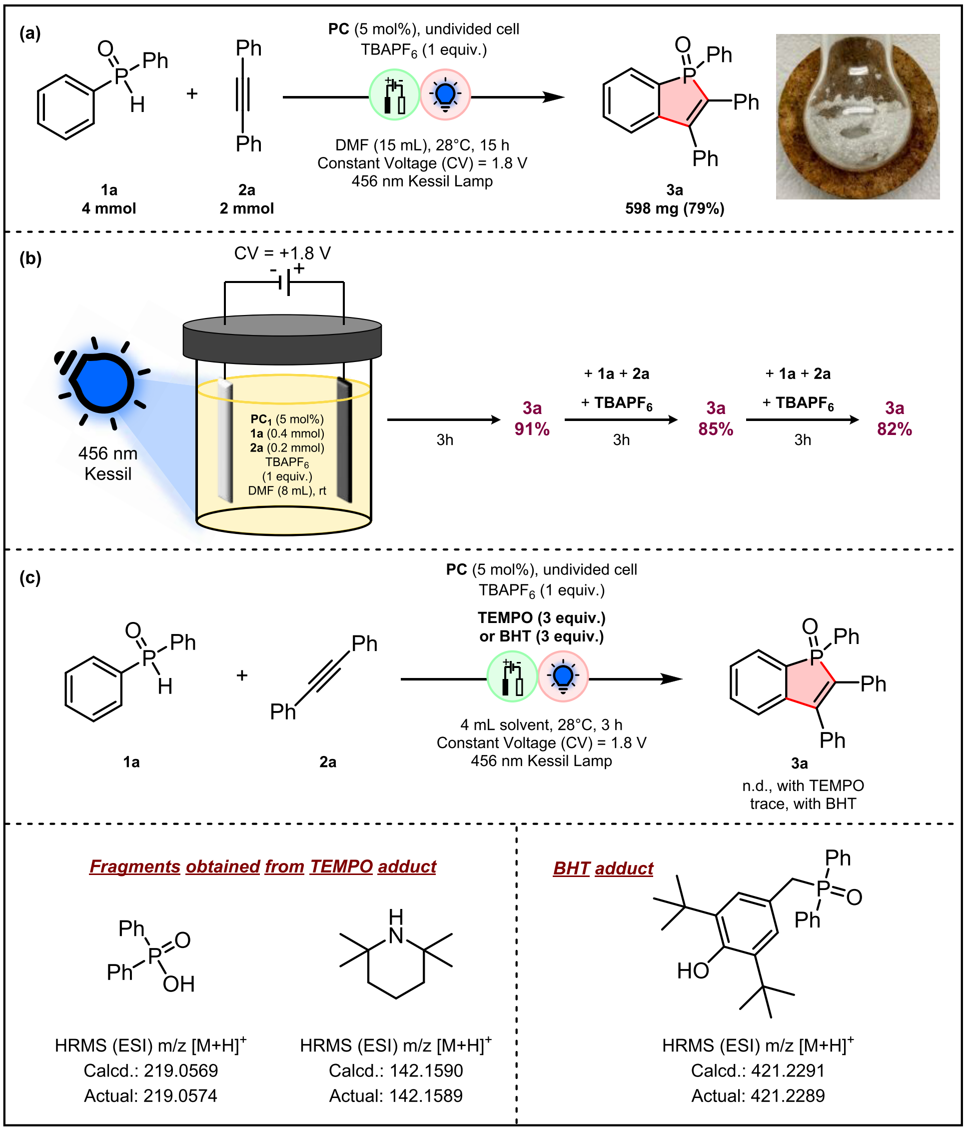

[a](a) Gram-scale reaction, (b) one-pot batch scale-up of **3a** (sustainability of **PC$_1$** and recyclability of electrodes), (c) radical scavenging experiments.

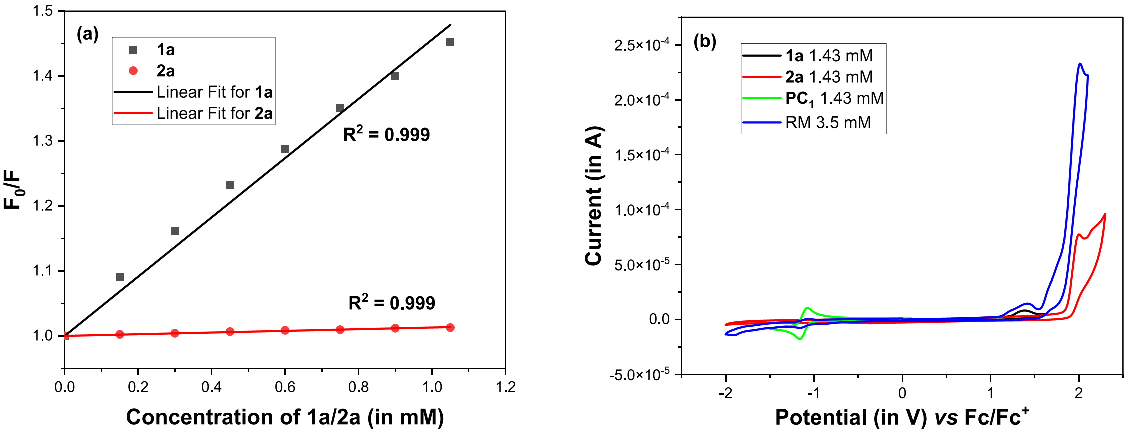

Figure 1. (a) Stern–Volmer plots for the fluorescence quenching of **PC$_1$** with **1a** (black line) and **2a** (red line). (b) Cyclic voltammetric plots of the starting materials **1a** (black trace), **2a** (red trace), **PC$_1$** (green trace), and the reaction mixture (blue trace).

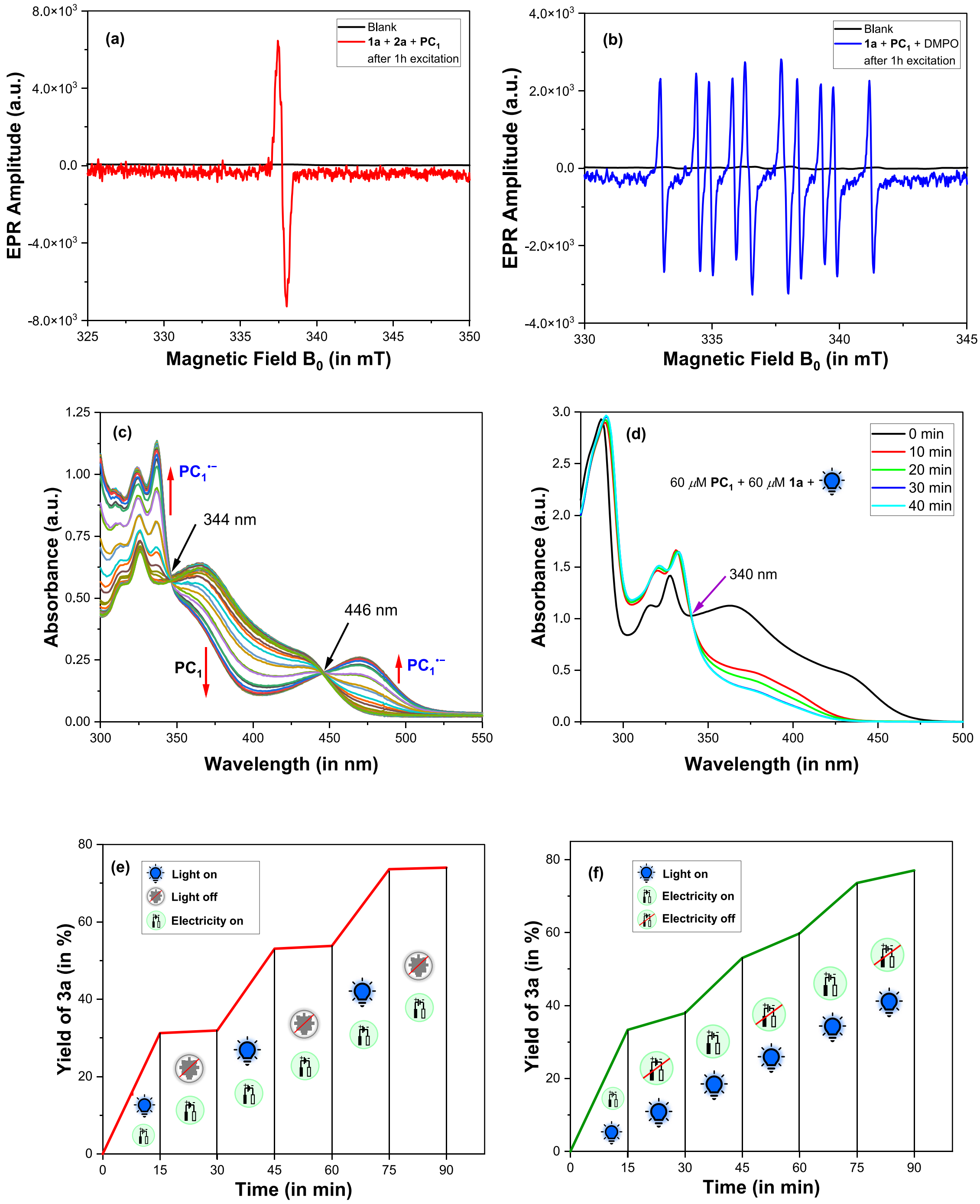

Figure 2. (a) EPR analysis of the reaction mixture. (b) EPR analysis of the phosphinoyl radical trapped with DMPO. (c) In situ spectroelectrochemical UV−vis data for reversible 1e$^-$ reduction of **PC$_1$**. (d) UV−vis spectra of a 1:1 mixture of **PC$_1$** and **1a** under intervals of light irradiation. (e) Light on−off experiment. (f) Electricity on−off experiment.

propargylic alcohols and alkynones were found to be suitable for our transformation and delivered good yields of the products (**4u**, 68%; **4v**, 74%). However, phenylacetylene and enynes did not provide the desired product under our optimized conditions. The regioselectivity of the products was governed by the stability of the alkenyl radical intermediate formed during the PEC process (vide infra).

We scaled the standard reaction to 10 times (Scheme 2a) and obtained an excellent yield of the intended product **3a** (598 mg, 79%). In addition, the photocatalyst 4CzIPN was recycled through single catalyst loading for a one-pot batch scale-up using the same electrodes. For this, we performed the first batch of the photoelectrochemical reaction with **1a** (0.4 mmol), **2a** (0.2 mmol), **PC$_1$** (5 mol %), and TBAPF$_6$ (1 equiv) in 8 mL of DMF for 3 h. Then, we introduced a further 0.4 mmol of **1a**, 0.2 mmol of **2a**, and electrolyte (20 mol %) and ran the second batch of the reaction. The successive addition of the third batch of reactants was done, and the reaction was performed until completion, giving after 9 h the desired product **3a** in 82% yield (Scheme 2b).

To support the proposed mechanism, we performed some controlled experiments. We noted that the model reaction was completely suppressed when performed along with radical

Scheme 3. Plausible Mechanism for the Photoelectrochemical Dehydrogenative Annulation

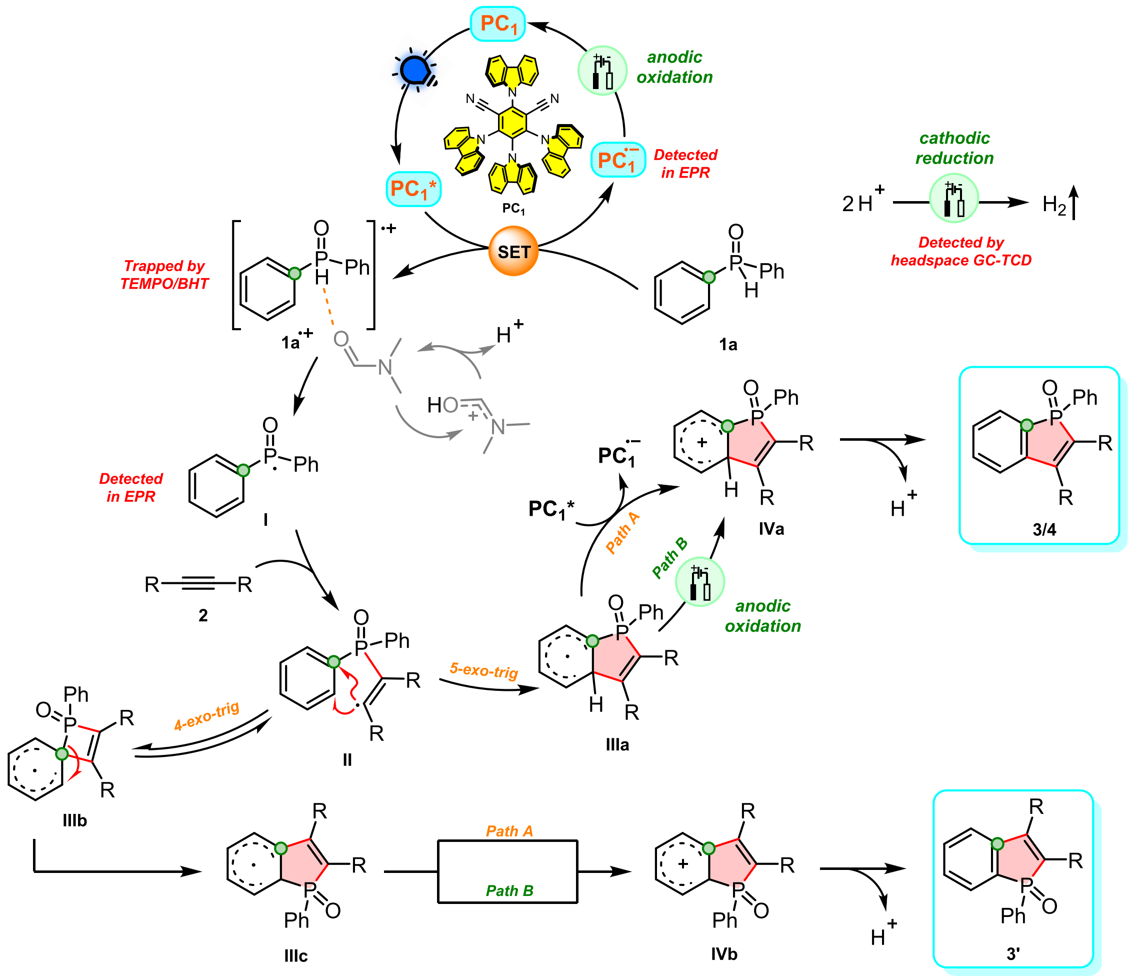

scavengers, namely, 2,2,6,6-tetramethylpiperidin-1-yl-oxidanyl (TEMPO) and 2,6-di-*tert*-butyl-4-methylphenol (BHT). The BHT-adduct and TEMPO-adduct fragments of diphenylphosphine oxide were detected in HRMS, thereby validating the radical intermediacy of the reaction (Scheme 2c).[15]

To gain more insight into the mechanistic details of our scheme, we recorded the UV−vis spectra of **PC$_1$** and the starting materials. We could not find any relevant ground-state interaction between **PC$_1$** with **1a**/**2a** (see the SI). Then, we measured the steady-state emission spectra of **PC$_1$** and observed fluorescence quenching by stepwise addition of the reactants to a 1.5 μM solution of **PC$_1$** excited at 450 nm. From the resulting Stern−Volmer plot, it was evident that **1a** was the primary static quencher (Figure 1a) and that a reductive quenching pathway between **PC$_1$** and **1a** can be formulated. Furthermore, the cyclic voltammetric studies (Figure 1b) disclosed that **PC$_1$** ($E_{1/2}$* = +1.49 V vs SCE) can photo-oxidize **1a** ($E_{p,a}$ = 1.21 V vs SCE) to furnish radical ion pairs **PC$_1$**$^{\bullet-}$ and **1a**$^{\bullet+}$ (see the SI). These radicals were also examined via EPR measurements of the reaction mixture to obtain **PC$_1$**$^{\bullet-}$ (g = 2.004) and DMPO (5,5-dimethyl-1-pyrroline-*N*-oxide) trapped **1a**$^{\bullet+}$ (Figure 2a,b).[14] These hypotheses were supported by the spectroelectrochemical data from 1e$^-$ reduction of **PC$_1$** (Figure 2c) and UV−vis analyses of a 1:1 mixture of **PC$_1$** and **1a** under constant intervals of light irradiation where the isosbestic point near 340 nm reveals the formation of the radical ion pairs (Figure 2d). Light on−off and electricity on−off experiments were performed to validate the continuous prerequisite roles of both light irradiance and a constant supply of electricity through constant voltage mode throughout the reaction (Figure 2e,f).

Based on the spectroscopic studies and the controlled experiments, we were able to delineate in detail a plausible mechanistic picture (Scheme 3). Initially, photoexcited **PC$_1$*** oxidizes **1a** by a single electron transfer (SET) process. The key role of electricity comes into action by regenerating the active form of catalyst **PC$_1$** by anodic oxidation of **PC$_1$**$^{\bullet-}$. **1a**$^{\bullet+}$, thus formed gets deprotonated in situ by the solvent, as DMF can act as a weak base to generate the stable double benzylic *P*-centered radical intermediate **I**. Then, alkynes **2** react with **I** to produce the second alkenyl radical intermediate **II**. In the case of unsymmetrical alkynes, the more stable alkenyl radical with resonance stabilization is formed regioselectively. The fate of **II** lies in either 5-*exo-trig* or 4-*exo-trig* cyclizations. The delocalized cyclohexadienyl radical intermediate **IIIa** is formed upon 5-*exo-trig* cyclization which is further oxidized to cationic intermediate **IVa** either by the excited photocatalyst (Path A) or through anodic oxidation (Path B). The reversible 4-*exo-trig* cyclization of **II** on the *ipso*-carbon atom results in the formation of spirocyclohexadienyl radical intermediate **IIIb** which can either revert back to **II** based on the steric nature of the substituents present in the *P*-aryl rings or can undergo ring expansion to form the radical intermediate **IIIc** which gets oxidized in a similar fashion to that of **IIIa** to produce the cationic intermediate **IVb**. Subsequent deprotonation and rearomatization of **IVa**/**b**

Scheme 4. Intermolecular Competition and Kinetic Isotopic Experiments[a]

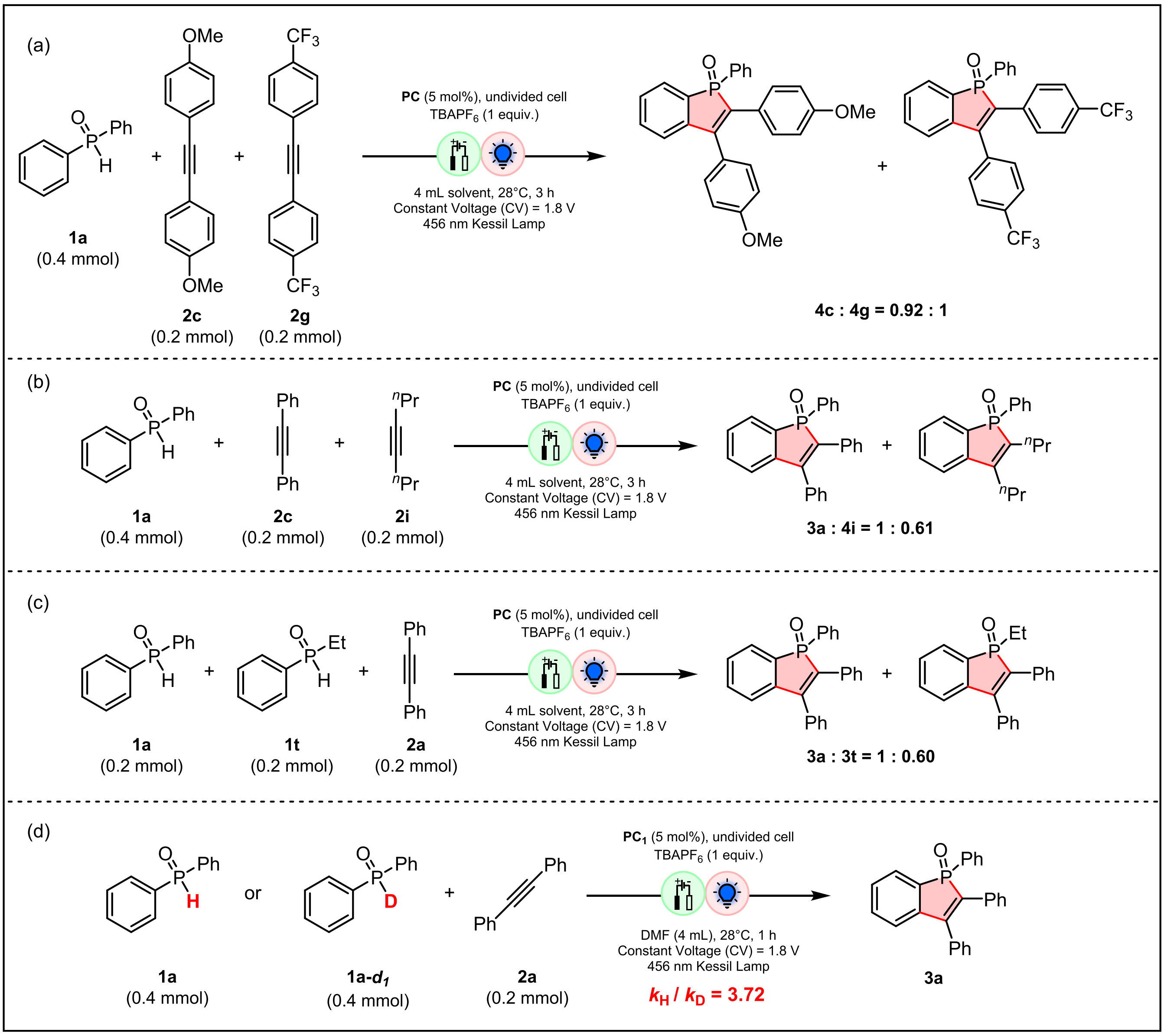

[a] (a) Intermolecular competition between electron-rich and electron-deficient alkynes. (b) Intermolecular competition between aromatic and aliphatic substituted alkynes. (c) Intermolecular competition between diarylphosphine oxide and alkyl arylphosphine oxide. (d) Kinetic isotopic experiment.

furnish the desired benzo[*b*] phosphole oxide products **3**, **3′**, or **4**. To maintain the electrical neutrality of the solution, protons are reduced in the cathode to produce H_2 gas which was detected by GC-TCD analysis of the reaction mixture headspace (see the SI). The regioisomeric ratios of the products in the scope of substituted diarylphosphine oxides indicate that the 5-*exo-trig* cyclization of **II** is the dominant pathway in the major cases. However, in the case of the phosphine oxides having *ortho*-substituents on the *P*-aryl rings (**3c**, **3i**), the formation of the intermediate **IIIa** would suffer from steric repulsions, which in turn can be avoided on the formation of the spirocyclohexadienyl radical intermediate **IIIb**, hence preferring the 4-*exo-trig* pathway to produce the other regioisomer selectively in excess.

Intermolecular competitive photoelectrochemical annulations were performed with alkynes and phosphine oxides, specifically with different electronic properties. Electron-rich **2c** and electron-deficient **2g** furnished similar yields of respective products, while **2c** and **2i** in competition formed **3a** predominantly over **4i**. Diarylphosphine oxide **1a** dominated over alkyl arylphosphine oxide **1t** to produce **3a** as the major product (Scheme 4a,c). Kinetic isotopic studies reveal that the formation of a phosphinoyl radical is involved in the rate-determining step. The ratio of k_H/k_D was found to be 3.72, when the standard reaction was performed with deuterodiphenylphosphine oxide (**1a**-d_1) which indicates a primary kinetic isotopic effect (Scheme 4d).[16]

The benzo[*b*]phosphole oxide products have attracted attention in their applications in organic light-emitting diodes (OLEDs), organic photovoltaic solar cells (OPVs), cell imaging dyes, fluorescent probes, and block copolymers. The synthesized products **3a**, **4j**, **4k**, and **4l** are some of the most common examples, demonstrating the synthetic value and practical applicability of this PEC methodology. The photophysical properties of some of the products were determined for their applications (see the SI).

CONCLUSIONS

In summary, we have established a sustainable and scalable photoelectrochemical strategy to construct diverse benzo[*b*]-phosphole oxides by eliminating the conventional use of stoichiometric transition-metal oxidants, sacrificial additives, and bases. The photocatalytic pathway triggers a radical mechanism that initiates an intermolecular SET between the organophotocatalyst 4CzIPN and secondary phosphine oxides. Electrochemistry serves as a greener oxidant. Moreover, detailed mechanistic investigations based on cyclic voltammetry, spectroelectrochemistry, fluorescence quenching, EPR spectroscopic, and kinetic isotopic studies experimentally support the proposed reaction pathway. A wide functional group tolerance and a one-pot batch scale-up were observed due to the reusability of the photocatalyst and the electrodes. The fusion of PRC and SOE for sequential P−H/C−H functionalization was achieved, allowing a simpler protocol to synthesize benzo[*b*]phosphole oxides, a class of molecules with eminent importance in the domain of material science.

MATERIALS AND METHODS

Materials. The chemicals were obtained from commercial sources and were used as received unless otherwise specified (see the SI for more details).

Methods. An oven-dried ElectraSyn vial (5 mL) equipped with a magnetic stirring bar was charged with secondary phosphine oxide **1** (0.4 mmol, 2.0 equiv), alkyne **2** (0.2 mmol, 1.0 equiv), **PC$_1$** (5 mol %, 0.01 mmol), and TBAPF$_6$ (0.2 mmol, 1.0 equiv). Exactly 4 mL of DMF was added to the ElectraSyn vial. An ElectraSyn vial cap equipped with Graphite SK-50 as an anode and IKA Platinum foil as a cathode was fitted tightly to the reaction vial. The reaction mixture was then stirred vigorously for 10 min to make the mixture homogeneous. The reaction mixture was simultaneously electrolyzed for 3 h by applying 1.8 V constant potential with 1200 rpm magnetic stirring under irradiation with a Kessil PR160−456 nm lamp. After completion of the reaction, the reaction mixture was extracted and purified by column chromatography (see the SI for more details).

ASSOCIATED CONTENT

Supporting Information

The Supporting Information is available free of charge at https://pubs.acs.org/doi/10.1021/acscatal.4c06292.

> Experimental details and characterization data which includes NMR spectra of all of the products, spectroscopic and cyclic voltammetric details, and corresponding figures (PDF)

AUTHOR INFORMATION

Corresponding Author

Burkhard König − *Institute of Organic Chemistry, Faculty of Chemistry and Pharmacy, University of Regensburg, D-93053 Regensburg, Germany;* orcid.org/0000-0002-6131-4850; Email: burkhard.koenig@ur.de

Author

Nayan Saha − *Institute of Organic Chemistry, Faculty of Chemistry and Pharmacy, University of Regensburg, D-93053 Regensburg, Germany;* orcid.org/0009-0008-1688-8637

Complete contact information is available at: https://pubs.acs.org/10.1021/acscatal.4c06292

Author Contributions

B.K. and N.S. conceived the idea. N.S. performed the experiments and prepared the Supporting Information. The manuscript was written through the contributions of all authors. All authors have given approval to the final version of the manuscript.

Notes

The authors declare no competing financial interest.

ACKNOWLEDGMENTS

This work was supported by the Deutsche Forschungsgemeinschaft [DFG (German Science Foundation) grant TRR 325-444632635]. The authors thank Regina Hoheisel (University of Regensburg) for her assistance in cyclic voltammetric experiments and Dr. Rudolf Vasold (University of Regensburg) for his assistance in GC-MS measurements.

REFERENCES

(1) (a) Brown, D. M.; Clark, B. F. C.; Letters, R. Phospholipids. Part VII. The structure of a monophosphoinositide. *J. Chem. Soc.* **1961**, 3774−3779. (b) Inch, T. D. The Biological Importance of Organophosphorus Compounds Containing a Carbon-phosphorus Bond. *Novartis Found. Symp.* **1978**, *57*, 135−153. (c) Neog, K.; Gogoi, P. Recent advances in the synthesis of organophosphorus compounds via Kobayashi's aryne precursor: a review. *Org. Biomol. Chem.* **2020**, *18*, 9549. (d) Demkowicz, S.; Rachon, J.; Daśko, M.; Kozak, W. Selected organophosphorus compounds with biological activity. Applications in medicine. *RSC Adv.* **2016**, *6*, 7101. (e) Singh, B. K.; Walker, A. Microbial degradation of organophosphorus compounds. *FEMS Microbiol. Rev.* **2006**, *30*, 428−471. (f) Wei, G.-L.; Li, D.; Zhuo, M.; Liao, Y.; Xie, Z.; Guo, T.; Li, J.; Zhang, S.; Liang, Z. Organophosphorus flame retardants and plasticizers: Sources, occurrence, toxicity and human exposure. *Environ. Pollut.* **2015**, *196*, 29−46.

(2) (a) Kolodiazhna, A. O.; Kolodiazhnyi, O. I. Chiral Organophosphorus Pharmaceuticals: Properties and Application. *Symmetry* **2023**, *15*, 1550. (b) Stolar, M.; Baumgartner, T. Phosphorus-Containing materials for organic electronics. *Chem. - Asian J.* **2014**, *9*, 1212−1225. (c) Kamer, P. C. J.; van Leeuwen, P. W. N. M.; Reek, J. N. H. Wide Bite Angle Diphosphines: Xantphos Ligands in Transition Metal Complexes and Catalysis. *Acc. Chem. Res.* **2001**, *34*, 895−904. (d) Horsman, G. P.; Zechel, D. L. Phosphonate Biochemistry. *Chem. Rev.* **2017**, *117*, 5704−5783. (e) Baumgartner, T.; Réau, R. Organophosphorus π-Conjugated Materials. *Chem. Rev.* **2006**, *106*, 4681−4724. (f) Peruzzini, M.; Gonsalvi, L., Ed. *Phosphorus Compounds: Advanced Tools in Catalysis and Material Sciences*; Springer: Berlin, 2011.

(3) (a) Matano, Y.; Saito, A.; Fukushima, T.; Tokudome, Y.; Suzuki, F.; Sakamaki, D.; Kaji, H.; Ito, A.; Tanaka, K.; Imahori, H. Fusion of Phosphole and 1,1′-Biacenaphthene: Phosphorus(V)-Containing Extended π-Systems with High Electron Affinity and Electron Mobility. *Angew. Chem., Int. Ed.* **2011**, *50*, 8016−8020. (b) Fave, C.; Cho, T.-Y.; Hissler, M.; Chen, C.-W.; Luh, T.-Y.; Wu, C.-C.; Réau, R. First Examples of Organophosphorus-Containing Materials for Light-Emitting Diodes. *J. Am. Chem. Soc.* **2003**, *125*, 9254−9255. (c) Su, H.-C.; Fadhel, O.; Yang, C.-J.; Cho, T.-Y.; Fave, C.; Hissler, M.; Wu, C.-C.; Réau, R. Toward Functional π-Conjugated Organo-phosphorus Materials: Design of Phosphole-Based Oligomers for Electroluminescent Devices. *J. Am. Chem. Soc.* **2006**, *128*, 983−995. (d) Taki, M.; Ogasawara, H.; Osaki, H.; Fukazawa, A.; Sato, Y.; Ogasawara, K.; Higashiyama, T.; Yamaguchi, S. A red-emitting ratiometric fluorescent

probe based on a benzophosphole P-oxide scaffold for the detection of intracellular sodium ions. *Chem. Commun.* **2015**, *51*, 11880−11883. (e) Parke, S. M.; Tanaka, S.; Yu, H.; Hupf, E.; Ferguson, M. J.; Zhou, Y.; Naka, K.; Rivard, E. Highly fluorescent benzophosphole Oxide Block-Copolymer micelles. *Macromolecules* **2019**, *52*, 7477−7488.

(4) (a) Baba, K.; Tobisu, M.; Chatani, N. Palladium-Catalyzed Direct Synthesis of Phosphole Derivatives from Triarylphosphines through Cleavage of Carbon−Hydrogen and Carbon−Phosphorus Bonds. *Angew. Chem., Int. Ed.* **2013**, *52*, 11892−11895. (b) Xu, S.; Nishimura, K.; Saito, K.; Hirano, K.; Miura, M. Palladium-catalysed C−H arylation of benzophospholes with aryl halides. *Chem. Sci.* **2022**, *13*, 10950−10960. (c) Tsuji, H.; Sato, K.; Ilies, L.; Itoh, Y.; Sato, Y.; Nakamura, E. Modular Synthesis of Benzo[*b*]phosphole Derivatives via BuLi-Mediated Cyclization of (*o*-Alkynylphenyl)phosphine. *Org. Lett.* **2008**, *10*, 2263−2265. (d) Sanji, T.; Shiraishi, K.; Kashiwabara, T.; Tanaka, M. Base-Mediated Cyclization Reaction of 2-Alkynylphenylphosphine Oxides: Synthesis and Photophysical Properties of Benzo[*b*]phosphole Oxides. *Org. Lett.* **2008**, *10*, 2689−2692. (e) Wu, B.; Yoshikai, N. Recent developments in synthetic methods for benzo[*b*]heteroles. *Org. Biomol. Chem.* **2016**, *14*, 5402−5416.

(5) (a) Chen, Y.-R.; Duan, W. Silver-Mediated Oxidative C−H/P−H Functionalization: An Efficient Route for the Synthesis of Benzo[b]phosphole Oxides. *J. Am. Chem. Soc.* **2013**, *135*, 16754−16757. (b) Unoh, Y.; Hirano, K.; Satoh, T.; Miura, M. An Approach to Benzophosphole Oxides through Silver- or Manganese-Mediated Dehydrogenative Annulation Involving C-C and C-P Bond Formation. *Angew. Chem., Int. Ed.* **2013**, *52*, 12975−12979. (c) Ackermann, L.; Ma, W. Silver-Mediated alkyne annulations by C−H/P−H functionalizations: Step-Economical access to benzophospholes. *Synthesis* **2014**, *46*, 2297−2304. (d) Zhang, P.; Gao, Y.; Zhang, L.; Li, Z.; Liu, Y.; Tang, G.; Zhao, Y. Copper-Catalyzed Cycloaddition between Secondary Phosphine Oxides and Alkynes: Synthesis of Benzophosphole Oxides. *Adv. Synth. Catal.* **2016**, *358*, 138−142. (e) Ma, L.; Mallet-Ladeira, S.; Monot, J.; Martin-Vaca, B.; Bourissou, D. Efficient synthesis of benzophosphole oxides by Ag-Promoted radical cycloisomerization. *Org. Chem. Front.* **2024**, *11*, 3376.

(6) Sluggett, G. W.; Turro, C.; George, M. W.; Koptyug, I. V.; Turro, N. J. (2,4,6-Trimethylbenzoyl)diphenylphosphine Oxide Photochemistry. A Direct Time-Resolved Spectroscopic Study of Both Radical Fragments. *J. Am. Chem. Soc.* **1995**, *117*, 5148−5153.

(7) Quint, V.; Morlet-Savary, F.; Lohier, J.; Lalevée, J.; Gaumont, A.; Lakhdar, S. Metal-Free, Visible Light-Photocatalyzed Synthesis of Benzo[*b*]phosphole Oxides: Synthetic and Mechanistic Investigations. *J. Am. Chem. Soc.* **2016**, *138*, 7436−7441.

(8) (a) Roth, H. D. The Beginnings of Organic Photochemistry. *Angew. Chem., Int. Ed.* **1989**, *28*, 1193−1207. (b) Prier, C. K.; Rankic, D. A.; MacMillan, D. W. C. Visible Light Photoredox Catalysis with Transition Metal Complexes: Applications in Organic Synthesis. *Chem. Rev.* **2013**, *113*, 5322−5363. (c) Marzo, L.; Pagire, S. K.; Reiser, O.; König, B. Visible-Light Photocatalysis: Does It Make a Difference in Organic Synthesis? *Angew. Chem., Int. Ed.* **2018**, *57*, 10034−10072. (d) Skubi, K. L.; Blum, T. R.; Yoon, T. P. Dual Catalysis Strategies in Photochemical Synthesis. *Chem. Rev.* **2016**, *116*, 10035−10074. (e) Douglas, J. J.; Sevrin, M. J.; Stephenson, C. R. J. Visible Light Photocatalysis: Applications and New Disconnections in the Synthesis of Pharmaceutical Agents. *Org. Process Res. Dev.* **2016**, *20*, 1134−1147. (f) Matsui, J. K.; Lang, S. B.; Heitz, D. R.; Molander, G. A. Photoredox-Mediated Routes to Radicals: The Value of Catalytic Radical Generation in Synthetic Methods Development. *ACS Catal.* **2017**, *7*, 2563−2575. (g) Speckmeier, E.; Fischer, T. G.; Zeitler, K. A toolbox approach to construct broadly applicable Metal-Free catalysts for photoredox chemistry: Deliberate tuning of redox potentials and importance of halogens in Donor−Acceptor Cyanoarenes. *J. Am. Chem. Soc.* **2018**, *140*, 15353−15365. (h) Singh, S.; Roy, V. J.; Dagar, N.; Sen, P. P.; Roy, S. R. Photocatalysis in Dual Catalysis Systems for Carbon-Nitrogen Bond Formation. *Adv. Synth. Catal.* **2021**, *363*, 937−979.

(9) (a) Yang, N. C.; Yang, D.-D. H. Photochemical reactions of ketones in solution. *J. Am. Chem. Soc.* **1958**, *80*, 2913−2914. (b) Woodward, R. B.; Hoffmann, R. Stereochemistry of Electrocyclic Reactions. *J. Am. Chem. Soc.* **1965**, *87*, 395−397. (c) Ischay, M. A.; Anzovino, M. E.; Du, J.; Yoon, T. P. Efficient Visible Light Photocatalysis of [2 + 2] Enone Cycloadditions. *J. Am. Chem. Soc.* **2008**, *130*, 12886−12887. (d) Nicewicz, D. A.; MacMillan, D. W. C. Merging Photoredox Catalysis with Organocatalysis: The Direct Asymmetric Alkylation of Aldehydes. *Science* **2008**, *322*, 77−80.

(10) (a) Zhu, C.; Ang, N. W. J.; Meyer, T. H.; Qiu, Y.; Ackermann, L. Organic Electrochemistry: Molecular Syntheses with Potential. *ACS Cent. Sci.* **2021**, *7*, 415−431. (b) Little, R. D. A Perspective on Organic Electrochemistry. *J. Org. Chem.* **2020**, *85*, 13375−13390. (c) Pollok, D.; Waldvogel, S. R. Electro-organic synthesis—a 21st century technique. *Chem. Sci.* **2020**, *11*, 12386−12400. (d) Yan, M.; Kawamata, Y.; Baran, P. S. Synthetic Organic Electrochemical Methods Since 2000: On the Verge of a Renaissance. *Chem. Rev.* **2017**, *117*, 13230−13319. (e) Kawamata, Y.; Baran, P. S. Electrosynthesis: Sustainability Is Not Enough. *Joule* **2020**, *4*, 701−704. (f) Moeller, K. D. Using Physical Organic Chemistry to Shape the Course of Electrochemical Reactions. *Chem. Rev.* **2018**, *118*, 4817−4833. (g) Heard, D. M.; Lennox, A. J. J. Electrode Materials in Modern Organic Electro-chemistry. *Angew. Chem., Int. Ed.* **2020**, *59*, 18866−18884. (h) Yuan, Y.; Yang, J.; Lei, A. W. Recent advances in electrochemical oxidative cross coupling with hydrogen evolution involving radicals. *Chem. Soc. Rev.* **2021**, *50*, 10058−10086. (i) Sandford, C.; Edwards, M. A.; Klunder, K. J.; Hickey, D. P.; Li, M.; Barman, K.; Sigman, M. S.; White, H. S.; Minteer, S. D. A Synthetic Chemist's Guide to Electroanalytical Tools for Studying Reaction Mechanisms. *Chem. Sci.* **2019**, *10*, 6404−6422. (j) Sen, P. P.; Dagar, N.; Singh, S.; Roy, V. J.; Pathania, V.; Roy, S. R. Probing the versatility of metallo-electro hybrid catalysis: enabling access towards facile C−N bond formation. *Org. Biomol. Chem.* **2020**, *18*, 8994−9017.

(11) (a) Studer, A.; Curran, D. P. The electron is a catalyst. *Nat. Chem.* **2014**, *6*, 765−773. (b) Luca, O. R.; Gustafson, J. L.; Maddox, S. M.; Fenwick, A. Q.; Smith, D. C. Catalysis by electrons and holes: formal potential scales and preparative organic electrochemistry. *Org. Chem. Front.* **2015**, *2*, 823−848.

(12) (a) Moutet, J.-C.; Reverdy, G. Photochemistry of Cation Radicals in Solution; Photoinduced Electron-Transfer Reactions between Alcohols and the *N*,*N*,*N*′,*N*′,-Tetraphenyl-*p*-Phenylenediamine Cation Radical. *J. Chem. Soc. Chem. Commun.* **1982**, 654−655. (b) Yan, H.; Hou, Z.-W.; Xu, H.-C. Photoelectrochemical C−H Alkylation of Heteroarenes with Organotrifluoroborates. *Angew. Chem., Int. Ed.* **2019**, *58*, 4592−4595. (c) Wang, F.; Stahl, S. S. Merging Photochemistry with Electro-chemistry: Functional-Group Tolerant Electrochemical Amination of C(sp3)-H Bonds. *Angew. Chem., Int. Ed.* **2019**, *58*, 6385−6390. (d) Huang, H.; Strater, Z. M.; Rauch, M.; Shee, J.; Sisto, T. J.; Nuckolls, C.; Lambert, T. H. Electrophotocatalysis with a Trisaminocyclopropenium Radical Dication. *Angew. Chem., Int. Ed.* **2019**, *58*, 13318−13322. (e) Kim, H.; Kim, H.; Lambert, T. H.; Lin, S. Reductive Electrophotocatalysis: Merging Electricity and Light to Achieve Extreme Reduction Potentials. *J. Am. Chem. Soc.* **2020**, *142*, 2087−2092. (f) Tian, X.; Karl, T. A.; Reiter, S.; Yakubov, S.; Vivie-Riedle, R.; König, B.; Barham, J. P. Electro-mediated PhotoRedox Catalysis for Selective C(sp3)-O Cleavages of Phosphinated Alcohols to Carbanions. *Angew. Chem., Int. Ed.* **2021**, *60*, 20817−20825. (g) Barham, J. P.; König, B. Synthetic photoelectrochemistry. *Angew. Chem., Int. Ed.* **2020**, *59*, 11732−11747. (h) Sen, P. P.; Saha, N.; Roy, S. R. Investigating the Potency of a Phenalenyl-Based Photocatalyst under the Photoelectrochemical Condition for Intramolecular C−S Bond Formation. *ACS Catal.* **2024**, *14*, 907−920. (i) Qian, L.; Shi, M. Contemporary photoelectrochemical strategies and reactions in organic synthesis. *Chem. Commun.* **2023**, *59*, 3487−3506.

(13) (a) Huang, W.; Byun, J.; Rörich, I.; Ramanan, C.; Blom, P. W. M.; Lu, H.; Wang, D.; Da Silva, L. C.; Li, R.; Wang, L.; Landfester, K.; Zhang, K. A. I. Asymmetric Covalent Triazine Framework for Enhanced Visible-Light Photoredox catalysis via Energy Transfer Cascade. *Angew. Chem., Int. Ed.* **2018**, *57*, 8316−8320. (b) Khrizanforova, V. V.; Kholin, K. V.; Khrizanforov, M. N.; Kadirov, M. K.; Budnikova, Y. H. Electrooxidative CH/PH functionalization as a novel way to synthesize benzo[*b*]phosphole oxides mediated by catalytic amounts of silver acetate. *New J. Chem.* **2018**, *42*, 930−935. (c) Ma, D.;

Chen, W.; Hu, G.; Zhang, Y.; Gao, Y.; Yin, Y.; Zhao, Y. $K_2S_2O_8$-mediated metal-free direct P−H/C−H functionalization: a convenient route to benzo[*b*]phosphole oxides from unactivated alkynes. *Green Chem.* **2016**, *18*, 3522−3526. (d) Liu, L.; Dong, J.; Yan, Y.; Yin, S.; Han, L.; Zhou, Y. Photoredox-catalyzed decarboxylative alkylation/cyclization of alkynylphosphine oxides: a metal- and oxidant-free method for accessing benzo[*b*]phosphole oxides. *Chem. Commun.* **2019**, *55*, 233−236. (e) Huang, M.; Huang, H.; You, M.; Zhang, X.; Sun, L.; Chen, C.; Mei, Z.; Yang, R.; Xiao, Q. Direct air-induced arylphosphinoyl radicals for the synthesis of benzo[b]phosphole oxides. *Green Chem.* **2024**, *26*, 295−299. (f) Liu, W.-Q.; Lei, T.; Zhou, S.; Yang, X.; Li, J.; Chen, B.; Sivaguru, J.; Tung, C.; Wu, L. Cobaloxime Catalysis: Selective Synthesis of Alkenylphosphine Oxides under Visible Light. *J. Am. Chem. Soc.* **2019**, *141*, 13941−13947.

(14) Liu, Y.; Chen, X.; Li, X.; Zhu, S.; Li, S.; Song, Y.; Qu, L.; Yu, B. 4CzIPN-^{t}Bu-Catalyzed Proton-Coupled electron transfer for photosynthesis of phosphorylated *N*-Heteroaromatics. *J. Am. Chem. Soc.* **2021**, *143*, 964−972.

(15) An alternative inhibition pathway may involve oxidized TEMPO and BHT either electrochemically or by the excited photocatalyst. The oxidized scavenger may trap the phosphine oxide inhibiting the progress of the reaction.

(16) Cai, C.-Y.; Lai, X.; Wang, Y.; Hu, H.; Song, J.; Yang, Y.; Wang, C.; Xu, H. Photoelectrochemical asymmetric catalysis enables site- and enantioselective cyanation of benzylic C−H bonds. *Nat. Catal.* **2022**, *5*, 943−951.